Biological Evaluation of Nanoemulsion and Selenium-containing Nanoparticles Utilizing Ginger Oil as Antimicrobial and Antioxidant Activity

Maryam Masoud AlAhwiti, Hanan Ali Alatawi ,* and Jayda G. Eldiasty

A sustainable green synthesis technique was employed to synthesize selenium-based nanoparticles (SeNPs) and a nanoemulsion (NE) from ginger oil (Gr). The nanoparticles were analyzed by DLS, UV-visible, and TEM techniques. The "emulsion inversion point" (EIP) method, a cornerstone of low-energy nanoemulsion (NE) production at constant temperature, was utilized. The liquid phases and surfactant choice determined whether a different mixing sequence was preferable. Using an oil-in-water (O/W) system, ginger oil was transformed into ginger nanoemulsion (Gr-NE). Gr-NE consists of dispersed immiscible phases containing kinetically stable droplets of a liquid phase, with sizes ranging from 36.6 to 51.1 nm. This technique resulted in a high surface area, excellent optical clarity, outstanding stability, and tunable rheology. An environmentally friendly method of synthesizing selenium-based nanoparticles (SeNPs@Gr) with particle sizes ranging from 64.2 to 90.6 nm was developed by utilizing ginger oil. Antimicrobial and antioxidant properties of all the components, as well as SeNPs@Gr, were evaluated. By synthesizing Gr-NE and SeNPs@Gr with minimal environmental impact and using renewable resources, this work achieved alignment with principles of the circular bioeconomy. In particular, the work contributes to Sustainable Development Goals 3 (Improving People's Health) and 12 (Encouraging Responsible Production and Consumption).

DOI: 10.15376/biores.21.2.3569-3592

Keywords: Green synthesis; Nanoemulsion; Selenium nanoparticles; Antimicrobial; Antioxidant

Contact information: Department of Biological Sciences, University College of Haqel, University of Tabuk, Tabuk, Saudi Arabia; (431002156@stu.ut.edu.sa), (halatwi@ut.edu.sa), (galdiasti@ut.edu.sa).
**Corresponding author: Hanan A. Alatawi, Email: halatwi@ut.edu.sa*

INTRODUCTION

Zingiber officinale Roscoe (ginger), a member of the family Zingiberaceae, is a medicinal plant with a long-standing history of use in traditional medical systems, including Traditional Chinese, Ayurvedic, and Unani (Tibb-Unani) medicine. Historically, ginger has been employed for the management of a wide range of conditions, such as musculoskeletal pain, gastrointestinal disorders (including cramps, diarrhea, and vomiting), sore throat, fever, hypertension, infectious diseases, helminthiasis, and neurological disorders, including dementia (Ali *et al.* 2008). Owing to its extensive ethnomedicinal use and broad therapeutic profile, *Z. officinale* has attracted substantial scientific interest. Numerous reviews have documented its widespread application as both a culinary spice and a medicinal herb, emphasizing its pharmacological properties and global relevance (Afzal *et al.* 2001; Chrubasik *et al.* 2005). Shukla and Singh (2007) examined the potential role of ginger-derived compounds in cancer-related research, while

Grzanna *et al.* (2005) investigated its anti-inflammatory effects. In addition, several studies have evaluated the efficacy of ginger in the management of post-operative nausea and vomiting (Chrubasik *et al.* 2005; Grzanna *et al.* 2005; Chaiyakunapruk *et al.* 2006; Shukla and Singh, 2007).

Although these studies illustrate the varied therapeutic potential of ginger, the majority have investigated its effects in traditional formulations, frequently concentrating on isolated applications. To address challenges associated with the stability, solubility, and bioavailability of ginger bioactives, contemporary nanotechnological methods, especially nanoemulsion-based systems, have garnered significant interest. Nanoemulsions are droplets of a liquid phase that are spread out in an immiscible phase and are stable in suspension. They are about 100 nm in size. This produces a range of fascinating properties, including a large surface area, excellent stability, outstanding optical clarity, and variable rheology (Tadros *et al.* 2004; Solans *et al.* 2005; Mason *et al.* 2006; McClements, 2011; Fryd and Mason 2012; Gupta *et al.* 2016). Nanoemulsions can enhance the bioavailability of bioactives (Sarker 2005; Shakeel *et al.* 2007; Kumar *et al.* 2008; Lovelyn *et al.* 2011; McClements 2011), which include medications, vitamins, nutraceuticals, supplements, and other compounds. Smart cosmetic products and functional foods can be developed using them. They can also be used to create advanced polymeric materials and template nanoparticles and produce medication nanocrystals by crystallizing active pharmaceutical ingredients (API). It is crucial to understand the concepts behind nanoemulsion generation and have an effective way to synthesize them if the goal is to use them in the listed applications. Nanoemulsions with surfactant or co-surfactant molecules stabilizing the interface can be broadly classified into three types: type (1) are oil/water nanoemulsions, which have oil droplets suspended in water (Shakeel *et al.* 2007; Lovelyn *et al.* 2011); type (2) are water/oil nanoemulsions, which contain oil droplets in a water phase; and type (3) are bi-continuous nanoemulsions, which have both oil and water droplets interspersed (Anton *et al.* 2008; Landfester 2009).

Selenium is a trace metal that has shown activity in lowering cellular oxidative stress and increasing efficacy against resistant bacteria. Selenium nanoparticles (SeNPs) excel due to their exceptional physicochemical features, which include a high surface area-to-volume ratio and improved reactivity (Manojlović-Stojanoski *et al.* 2022; Shinde and Desai 2022). Se helps protect cells by lowering oxidative stress and getting the immune system to work better. SeNPs show promise as possible medicines because they are more bioavailable, less harmful, and have stronger biological effects (Spyridopoulou *et al.* 2021; Liu *et al.* 2023). The formation and stabilization of nanoparticles, as well as their associated biological activity, are mediated by specific bioactive phytochemicals present in ginger essential oil. These include sesquiterpenes such as zingiberene, β-sesquiphellandrene, and β-bisabolene, in addition to phenolic constituents such as gingerols, shogaols, and paradols. These compounds possess functional groups that are capable of acting as reducing and capping agents, thereby facilitating nanoparticle synthesis and contributing to their antioxidant, anti-inflammatory, and antimicrobial activities (Ravi Kiran and Aruna 2010; Ramadan *et al.* 2022). Utilizing renewable and biocompatible ingredients, this strategy lessens the ecological imprint of standard synthesis techniques (Khan and Lee 2020). To enhance the biological efficacy and facilitate nanoparticle manufacturing, this approach makes use of the rich phytochemical components found in plant extracts, including terpenoids, tannins, phenolics, and flavonoids (Alrashdi *et al.* 2023). Records of SeNP production using *Bacillus subtilis* show that these nanoparticles have antibacterial potential (Diwu *et al.* 2021). The ability of SeNPs to interact with bacterial cells has been shown by their characterisation, leading to enhanced antibacterial effects (Khattab *et al.* 2021).

Moreover, SeNPs possess antifungal properties against *Aspergillus* and *Penicillium* (Al-Brakati *et al.* 2021; Abdallah *et al.* 2023). Therapeutic techniques aimed at alleviating oxidative stress should benefit greatly from SeNPs due to their ability to eliminate free radicals and enhance cellular antioxidant defenses (Elmaaty *et al.* 2022).

The process of making NE and selenium nanoparticles in the presence of ginger oil is detailed in this research. For antibacterial activity against gram-positive and gram-negative bacteria, the synthesized NE and SeNPs were tested using the agar well diffusion method. For antimicrobial efficacy, they were tested using both the agar well diffusion and poisoned plate methods. In addition, assays for hydrogen peroxide (H_2O_2) and DPPH radical scavenging were used to assess their antioxidant properties. This research advances plant-based nanotechnology in biomedical research by demonstrating the efficacy of NE and SeNPs as multifunctional agents against antibacterial and oxidative stress. It offers a sustainable strategy for nanoparticle synthesis.

EXPERIMENTAL

Materials

The ginger oil was sourced from the National Research Centre located in Dokki, Cairo, Egypt. It was cultivated in Egypt, and it was of 99.9% purity. The compounds used included selenious acid (H_2SeO_3) from Sigma Aldrich, polysorbate 80 (Tween 80) and sorbitan monooleate 60 (Span 60), also from Sigma Aldrich, 1,1-diphenyl-2-picryl-hydrazil (DPPH) sourced from Merck, and methanol from Sigma Aldrich. Nutrient agar medium (NA) is a general culture medium utilized for the isolation and growth of less fastidious microorganisms, as well as for establishing permanent cultures. It comprises the following components (g/L): yeast extract 2.0, peptone 5.0, meat extract 1.0, NaCl 5.0, agar 15.0, with a pH of 7.4 ± 0.2. The nutrient broth medium (NB) comprised the following components (g/L): yeast extract 2.0, peptone 5.0, meat extract 1.0, NaCl 5.0, with a pH of 7.4 ± 0.2. One set of samples included the following codes: (1-Gr-NE); (2-SeNPs@Gr); (3-SeNPs); (4-Ginger oil); and (5-Ginger oil/DMSO (1:1, v/v). These were placed in 100.0 mL sterile conical flasks. The tested pathogenic microbial strains consisted of Gram-negative bacteria: *Escherichia coli* (ATCC 25922) and *Helicobacter pylori* (ATCC 43526), as well as Gram-positive bacteria: *Bacillus cereus* (ATCC 6629) and *Staphylococcus aureus* (ATCC 6538). Additionally, the pathogenic fungus *Candida albicans* (ATCC 10231) was included.

Synthesis of Nanoemulsion

Ginger oil nanoemulsion (Gr-NE) was prepared using the spontaneous emulsify-cation method. Briefly, the oil phase consisted of ginger essential oil mixed with sorbitan monooleate 60 (Span 60) as the lipophilic surfactant, while polysorbate 80 (Tween 80) was used as the hydrophilic co-surfactant. The surfactants were blended with the oil phase at predetermined ratios under continuous magnetic stirring until a homogeneous mixture was obtained. This oil–surfactant mixture was then slowly added dropwise to distilled water (aqueous phase) under constant stirring at room temperature. The system was stirred for an additional specified period to allow complete emulsification and nanoemulsion formation. The resulting nanoemulsion was visually inspected for homogeneity and stored for further characterization.

Synthesis of Selenium Nanoparticles (SeNPs@Gr)

A conical flask was filled with 10 mL of ginger oil and 10 mL of DMSO. Selenious acid (H_2SeO_3, 0.128 g, 0.1 mmol) was dissolved in 90 mL of deionized water and agitated at 60°C. After that, ginger oil in DMSO was added drop by drop for an hour to create an in-situ suspension of selenium nanoparticles. The hue of the fluid shifted to red, indicating the creation of selenium nanoparticles. The present of metallic (zero valence) nanoparticles was further confirmed using a UV-spectrophotometer. Dynamic light scattering (DLS) with transmission electron microscopy (TEM) (Alkherb *et al.* 2024).

Spectroscopy

Using UV-VIS spectroscopy, the Shimadzu spectrophotometer tracked the development of selenium nanoparticles in ginger oil between 400 and 700 nm.

Transmission Electron Microscopy (TEM)

High-resolution transmission electron microscopy (HR-TEM; JEOL JEM-2100) was used to examine the SeNPs and nanoemulsion shape and nanoparticle size. The suspension solution was applied to a 400-mesh carbon-coated copper grid coated with an amorphous carbon support film (without Formvar) to prepare the TEM samples, and the solvent was allowed to evaporate at room temperature.

Dynamic Light Scattering (DLS)

A particle size analyzer (Nano-ZS, Malvern Instruments Ltd., UK) was utilized to determine the average particle size, size distribution, and zeta potential of the samples. Before doing an analysis of the size distribution and zeta potential, the sample was subjected to sonication for 10 to 20 min.

Thermodynamic Stability Studies

By exposing the generated nanoemulsion (NE) formulations to a range of various stress and temperature settings, their stability was examined. They were first incubated for three days at 4 °C, then for three more days at 45 °C, repeating this cycle three times. After centrifuging NEs for 30 min at 2800 g, the formulations that passed the preceding stages were kept in freeze-thaw cycles for three days at -20 °C and then for three days at 25 °C. Finally, after being spread out in two millilitres of water, all of the NEs that withstood the tests were examined for any signs of phase separation, creaming, or coalescence. Those that passed every test and continued to be stable were then selected for characterization (Fryd and Mason 2012; Gupta *et al.* 2016).

Gas Chromatography and Mass Spectrometry (GC-MS)

The GC-MS system used in this work was made by Agilent Technologies. The device was located at the Central Laboratories Network, National Research Centre in Giza, Egypt. It had a gas chromatograph (7890B) and a mass spectrometer detector (5977A). Comprising a film thickness of 0.25 μm and an internal diameter of 30 m by 0.25 mm, the HP-5MS column was attached to the gas chromatograph (GC). One splitless injection volume of 1.0 μL and the following temperature program were used for experiments. The carrier gas utilized in the analysis was hydrogen, and the flow rate in the analysis was 1.1 mL/min. The temperature was gradually raised from 40 °C for one min, then maintained at 200 °C for 1 min, 20 °C for 1 min, 220 °C for 1 min, and finally, 320 °C for 3 min. Both the injector and the detector were maintained at temperatures of 250 and 320 °C, respectively. The mass spectra were obtained by employing electron ionization (EI) at a

velocity of 70 electron volts, a mass-to-charge ratio (*m*/*z*) range of 50 to 550, and a solvent delay of 2.00 min. In the GC–MS analysis, the ion source (MS) temperature was maintained at 230 °C, while the quadrupole temperature was set at 150 °C. The spectrum fragmentation patterns were compared with the data stored in Wiley and the NIST Mass Spectral Library, which could lead to the identification of a great number of components.

Antimicrobial Activity

To determine the antibacterial activity of the prior samples, a battery of tests utilizing several human diseases was conducted. *Bacillus cereus*, *Staphylococcus aureus*, *Escherichia coli*, and *Helicobacter pylori* are examples of Gram-negative bacteria; *Candida albicans* is an example of a Gram-positive fungus that was utilized in the study. The infectious strains were freshly cultured in nutrient broth and incubated overnight at 37 °C, following the protocol described by Osman *et al.* (2015). Every plate that contained 25.0 mL of the sterile nutrient agar medium (NA) was inoculated with a 25.0 µL inoculum size of a different microorganism strain (Hafez *et al.* 2023). The samples (1-SeNPs@Gr, 2-Gr-NE, 3-SeNPs alone, 4-ginger oil) were made for each sample, and added one by one after the media had cooled and solidified. A well with a diameter of 0.6 cm was filled with 75.0 µL of the prior samples using the well diffusion method, which required a 0.6 cm cork borer (El-Masry *et al.* 2023). These inoculated plates were placed in the refrigerator for one hour to allow the samples to diffuse, followed by incubation at 37 ºC for 24 h. Zones of inhibition (ZI) were measured in mm (Tohamy *et al.* 2024).

The shake flask method was used for the second group to assess the antimicrobial activity of the tested strains. This was done by inoculating small conical flasks with 20.0 mL of nutrient broth medium and 25.0 µL of bacterial suspensions (0.5 McFarland standard, 1.5 × 108 CFU/mL). Separately, 100 µL of the tested sample was added to the inoculated flasks. The flasks were then incubated at 37 ºC for 24 h while being shaken using a vortex mixer at 120.0 rpm (Hamoda *et al.* 2022). For each strain, a sample-culture combination and a control flask had been serially diluted (10^{-1} to 10^{-4}). The petri-dishes holding solidified nutritional agar were inoculated with 100.0 µL of the 10^{-4} dilution of the investigated samples each to find the microbial inhibition. The following equation computed the decrease in growth, as a percentage *R* (%), for the treated samples against the control (untreated) samples (Hamoda *et al.* 2022),

$$\text{Relative Reduction (\%)} = (A - B)/B \times 100 \quad (1)$$

where *A* is CFU/mL determined in the untreated control sample, which contains pathogenic strains only without any treatment, and *B* is CFU/mL determined in the treated sample tested.

Antioxidant Activity

The free radical scavenging activity of the samples was evaluated using the 1,1-diphenyl-2-picrylhydrazyl (DPPH$^{\bullet}$) assay, following the method described by Shimada *et al.* (1992) with minor modifications (Badawy *et al.* 2019). A freshly prepared DPPH$^{\bullet}$ solution (0.1 mM) was obtained by dissolving DPPH in methanol. For each assay, 100 µL of the tested sample was mixed with 300 µL of the DPPH$^{\bullet}$ solution. The reaction mixture was vigorously shaken using a vortex mixer at approximately 2500 rpm for 30 s to ensure complete mixing. Each experiment was performed in triplicate. The mixtures were then incubated in the dark at room temperature, defined as 25 ± 1 °C, for 30 min to allow the reaction to reach equilibrium. Following incubation, the absorbance was measured at 517 nm using a microplate reader (*e.g.*, BioTek ELx800™, BioTek Instruments, USA).

Methanol containing DPPH• without a sample served as the control. A decrease in absorbance indicated higher free radical scavenging activity (El-Masry *et al.* 2023).

The DPPH radical scavenging activity was calculated using the following equation,

$$\text{DPPH scavenging effect (\%)} = \left(\frac{A_0 - A_1}{A_0}\right) \times 100 \quad (2)$$

where A_0 is the absorbance of the control reaction and A_1 is the absorbance in the presence of the sample (Oktay *et al.* 2009).

RESULTS AND DISCUSSION

Ginger Oil Nanoemulsion Preparation and Characterization (Gr-NE)

Gr-NE was prepared by an oil-in-water emulsification process. Polysorbate 80 and sorbitan monooleate 60 (5%, w/v) were dissolved in the aqueous phase, followed by the gradual addition of ginger oil under continuous high-shear homogenization until a homogeneous nanoemulsion was obtained (Fig. 1). Adding ginger oil to water with a surfactant caused the oil's hue to change from yellow to white. The presence of Gr-NE was confirmed by the transmission electron microscopy (TEM) investigation, as depicted in Fig. 2. This eco-friendly technique yields a spherical Gr-NE with an average particle size ranging from 36.6 to 51.1 nm and a small amount of aggregation.

Fig. 1. Preparation of ginger nanoemulsion

As shown in Fig. 3a, the particle size and surface charge of the graphene-based nanoemulsion (Gr-NE) were evaluated using dynamic light scattering (DLS) and zeta potential measurements. DLS analysis indicated an average hydrodynamic diameter of 195 nm with a polydispersity index (PDI) of 0.624 (Tables S1 and S3), suggesting a moderately broad size distribution. Transmission electron microscopy (TEM) revealed predominantly spherical particles with sizes ranging from 36.6 to 51.1 nm and an average particle size of 40.9 ± 6.8 nm. The observed discrepancy between TEM and DLS measurements can be attributed to the hydrodynamic diameter measured by DLS and the possible aggregation of particles in suspension. The zeta potential value of −33.3 mV indicates sufficient electrostatic repulsion, suggesting good colloidal stability of the Gr-NE system, consistent with previously reported studies (El Gohary *et al.* 2021; El-Sayed *et al.* 2022; Kamel *et al.* 2024).

- Mean size (TEM): 40.94 nm
- Standard deviation (SD): ±6.82 nm
- n = 4 measurements

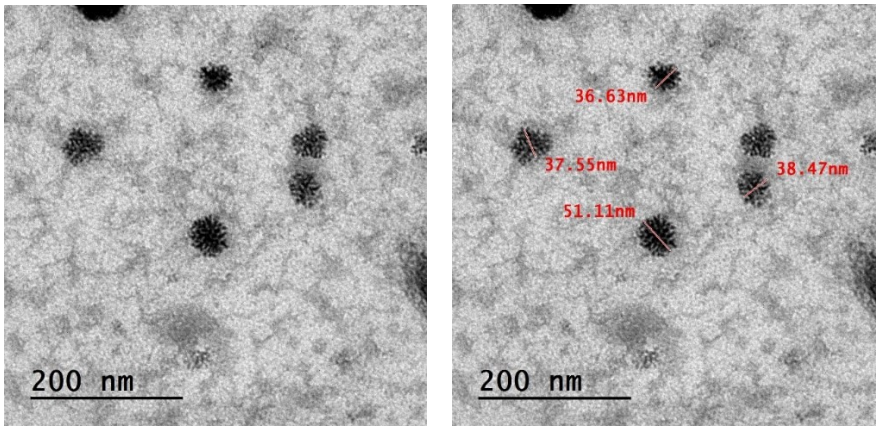

Fig. 2. TEM analysis of Gr-NE

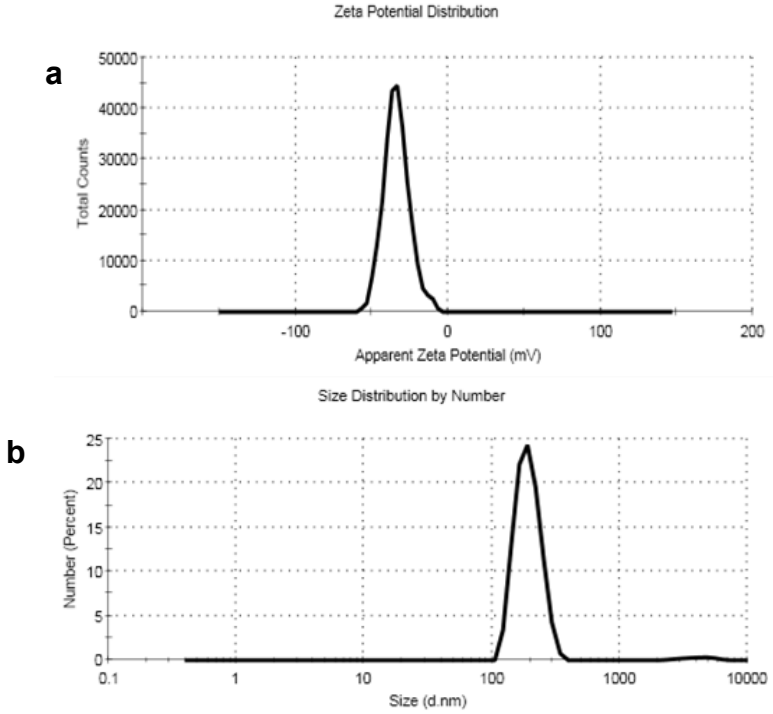

Fig. 3. (a) Particle size and (b) ZP of Gr-NE

Phyto-synthesis and Characterization of Selenium-containing Nanoparticles (SeNPs@Gr)

When analysing the phytochemicals in ginger oil, GC-MS was used to verify the presence of multiple distinct components. Alpha, epsilon-carotene-3,3'-diol, trans-beta-Ocimene, camphene, isoborneol, beta, benzene, 1-(1,5-dimethyl-4-hexenyl)-4-methyl-, and gingerol acetyl derivatives are all part of this formula (Fig. 4). Research has shown that ginger oil can effectively produce SeNPs due to its reducing and stabilizing properties. In order to synthesize SeNPs and maintain their stability, the Se^{+} cation was transformed to Se^{0} utilizing hydroxyl groups, which also served as oxygen sources. Selenium cations can be reduced by easily oxidizable phenolic and enolic structures, particularly those

present in gingerol, shogaol, and related phenylpropanoid derivatives in ginger oil. These compounds contain phenolic –OH groups conjugated with aromatic rings, which are well known to participate in redox reactions and to act as electron donors, unlike aliphatic alcohols (Jacob *et al.* 2007; Amini and Akbari 2019). The reaction between Se^{+} salt and ginger oil resulted in the production of SeNPs@Gr, which underwent a noticeable color change during the process.

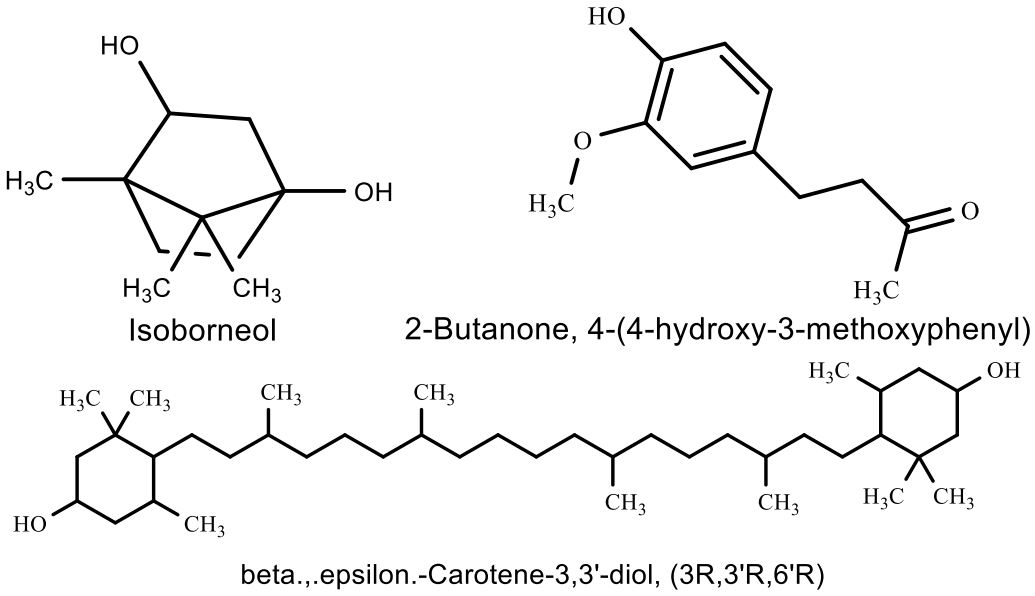

Fig. 4. The key phytochemical structures in the ginger oil

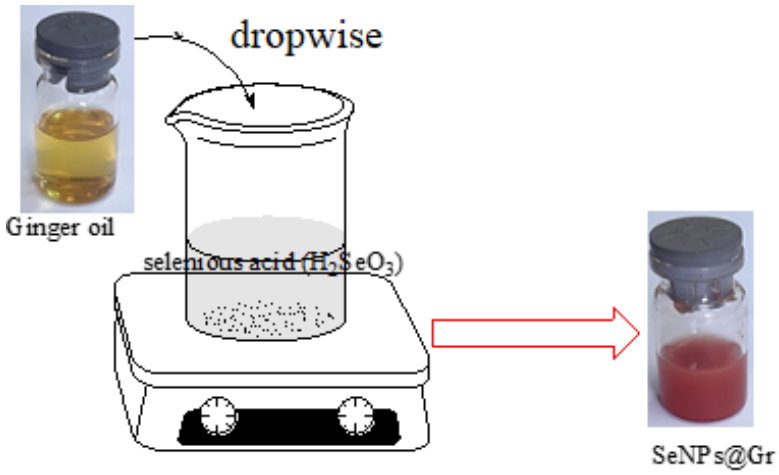

Fig. 5. Preparation of selenium nanoparticles using ginger oil (SeNPs@Gr)

The visual appearance of the reaction mixture before and after the incorporation of ginger oil into selenium nanoparticles (SeNPs@Gr) is shown in Fig. 5. The ginger oil initially exhibited a yellow coloration, which gradually changed to a deep crimson color after the addition of selenium salt and heating at approximately 60 °C for 24 h. This distinct color transformation indicates the formation of selenium nanoparticles (containing zero-valent metal) and is commonly associated with surface plasmon resonance effects. The synthesis of SeNPs was further monitored and confirmed using UV–Vis spectroscopy, as presented in Fig. S1.

Formation of selenium-based nanoparticles supported on graphene (SeNPs@Gr) was confirmed by TEM analysis (Fig. 6). The nanoparticles exhibited a predominantly spherical morphology with particle sizes ranging from 64.2 to 90.6 nm and an average size of 76.7 ± 14.3 nm, indicating slight aggregation. DLS analysis (Fig. 7a) showed an average hydrodynamic diameter of approximately 65 nm with a narrow size distribution. The difference between TEM and DLS results is attributed to the hydrodynamic nature of DLS measurements and possible dispersion effects in the colloidal system.

- Mean particle size (TEM): 76.73 nm
- Standard deviation (SD): ±14.32 nm

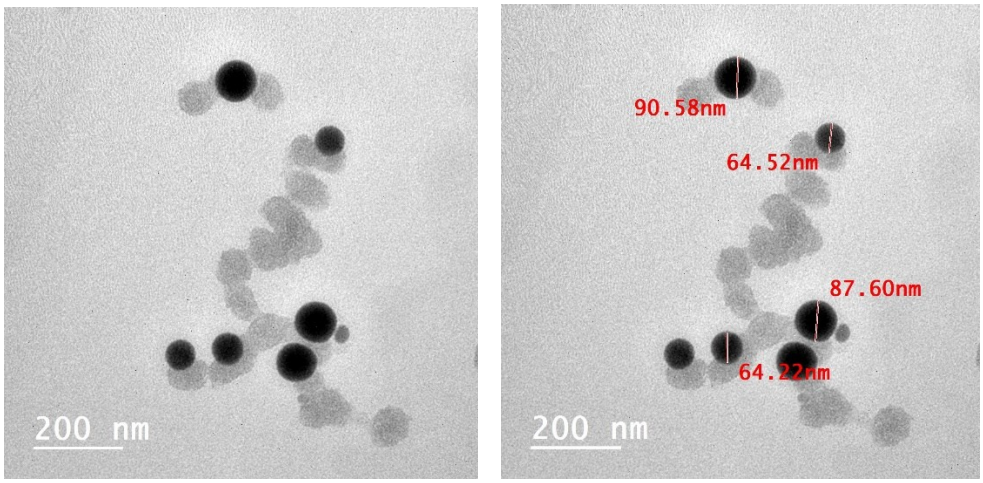

Fig. 6. (TEM) analysis of SeNPs@Gr

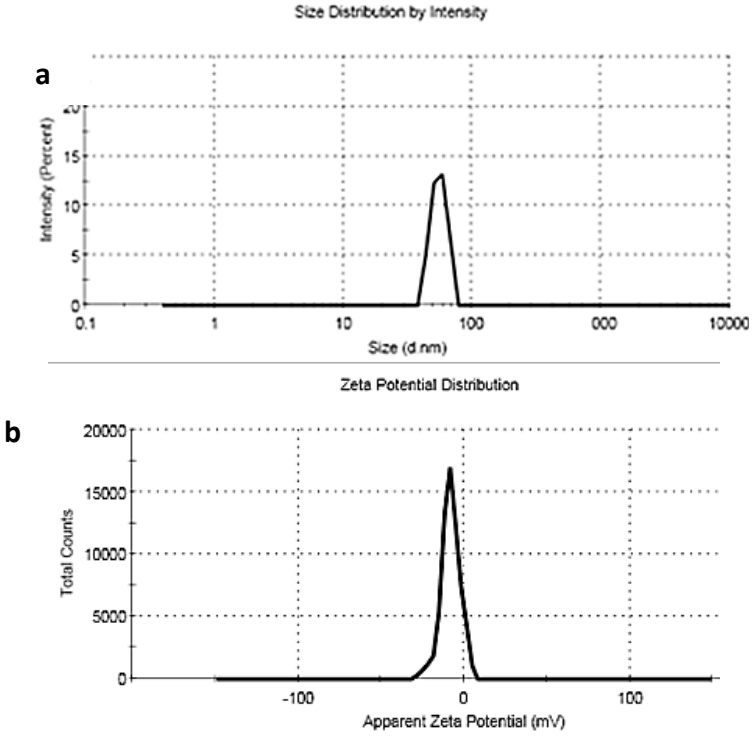

Fig. 7. SeNPs@Gr a) Particle size, & b) Zeta Potential

According to Tables S2 and S3, the PSA results showed an average hydrodynamic diameter of 55.7 nm for SeNPs@Gr with a PDI value of 0.528, indicating a moderately

broad particle size distribution. The zeta potential analysis (Fig. 7a,b) revealed a mean value of −8.05 mV with a wide distribution spanning both negative and positive values, including values near zero. This low absolute zeta potential suggests limited electrostatic stabilization, consistent with the observed aggregation behavior. The partial colloidal stability may be attributed to the presence of organic constituents associated with the graphene and bio-derived components, which can contribute to steric or electrosteric stabilization rather than charge-based repulsion.

GC-MS for Ginger Oil

Figure 8 shows a GC-MS chromatogram of several chemicals. The device's data library was used to identify them, and the match was greater than 72%. Table S4 (see Appendix) displays the eleven compounds that were identified, along with their retention durations and areas under the curves. There is also a breakdown of the proportion of each detected ingredient in the ginger oil. When considering the areas under the total curve, the highest percentages belonged to benzene, 1-(1,5-dimethyl-4-hexenyl)-4-methyl (α-curcumin) (36.8%), followed by (R)-1-methyl-4-(6-methylhept-5-en-2-yl)cyclohexa-1,4-diene (β-curcumin) (19.6%); 1H-benzocycloheptene, 2,4a,5,6,7,8,9,9a-octahydro-3,5,5-trimethyl-9-methylene-, (4aS-cis) (14.3%), beta.-longipinene (15.3%), gamma.-muurolene (6.3%), and camphene (3.4%).

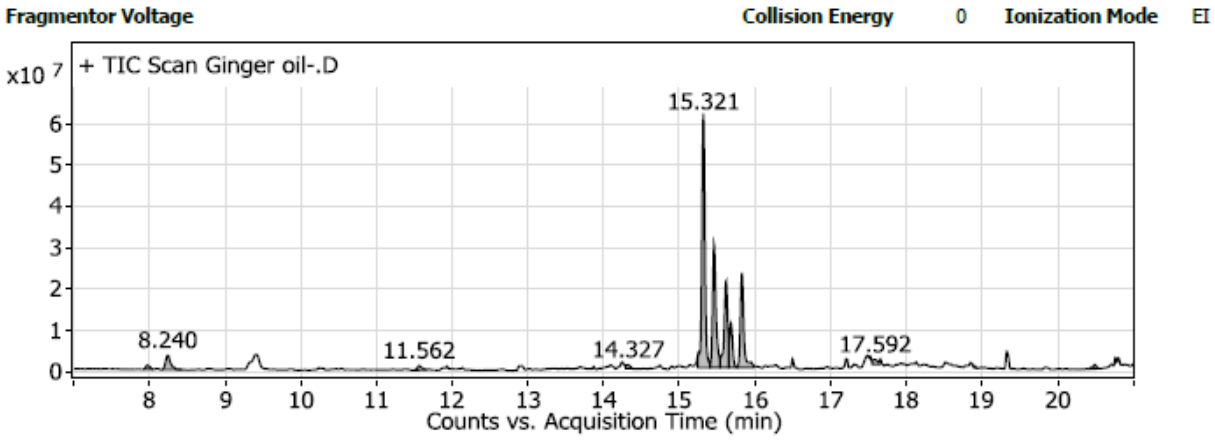

Fig. 8. GC-MS chromatogram of ginger oil

Antimicrobial Activity

Maybe the most significant medical breakthrough of the twentieth century was the development of effective, naturally occurring, and largely harmless antibacterial agents. Based on their site of activity, antimicrobial agents can inhibit cell wall synthesis, protein synthesis, nucleic acid synthesis, or disrupt cell membrane integrity; these four categories determine how antimicrobial agents work against pathogens that originate in plants, animals, or humans (El-Masry *et al.* 2023). Additionally, there were two primary groups into which the antimicrobial agents were classified.

The initial group of substances was categorized as bactericidal agents, meaning that they kill bacteria directly. This results in a 99.9 percent drop in the number of viable colony-forming units at a specific incubation time, typically 20 to 24 h (Montgomery and Kroeger 1984). The second group of agents was referred to as bacteriostatic agents because of their ability to suppress bacterial growth and reproduction without actually killing the bacteria (Balouiri *et al.* 2016; Bhargav *et al.* 2016).

By using the well diffusion method to measure the inhibition zone diameter, the samples coded [2-SeNPs@Gr & 5-ginger oil/DMSO, (1:1, v/v)] in Table 1, Fig. S2 demonstrate outstanding antimicrobial activity. These samples were applied to the Gram-positive bacteria *Staphylococcus aureus* and *Bacillus cereus*, as well as Gram-negative bacteria *Escherichia coli* and *Helicobacter pylori*, with inhibition zone ranges of 11 to 15 mm and 11 to 15 mm, respectively.

Table 1. Inhibition Zone Diameter (Millimeters) of the Samples

Bacteria	Treated sample					
	(1)	(2)	(3)	(4)	(5)	Reference** (CN)
Escherichia coli	NIL*	13.0	NIL	NIL	NIL	17.0
Helicobacter pylori	NIL	13.0	NIL	NIL	15.0	20.0
Bacillus cereus	NIL	11.0	NIL	NIL	13.0	20.0
Staphylococcus aureus	NIL	12.0	NIL	NIL	NIL	22.0

* Nil: - No antimicrobial activity recorded.
** Reference: -CN: Gentamicin 10 mcg (standard antibiotic disc) bioanalyze.

These two previous samples showed a bactericidal effect that destroyed and killed about 99% of total viable bacterial present in the culture. A shake flask method was used. The percentage reduction of colony forming units (CFU) was calculated in comparison to the previous tested pathogenic strains after applying the tested samples [2-SeNPs@Gr & 5-ginger oil/DMSO, (1:1, v/v)]. An excellent antimicrobial effect was recorded relative to all microbes. The % CFU reduction of Gram-positive bacteria *Staphylococcus aureus & Bacillus cereus* ranged from 96.2 to 99.9%. For Gram-negative bacteria *Escherichia coli & Helicobacter pylori* the reductions ranged from 93.8 to 99.2%. These results allow these samples to be classified as bactericidal agents that can reduce and kill more than 99.0 % of the previous bacterial count used in this experiment (Table 2, Fig. S3, Fig. S4). Also, the other samples [1-Gr-NE, 3-SeNPs only & 4-ginger oil] had a bacteriostatic effect, which refers to agents that can inhibit the growth or reproduction of bacteria and reduce the total viable bacterial count without necessarily killing or destroying them completely.

Table 2. Percentage Reduction in Colony-Forming Units (CFU) of Bacterial Strains Following Incubation, as Determined by the Shake Flask Method

Test Bacteria		Treated sample				
		(1)	(2)	(3)	(4)	(5)
1-	*Escherichia coli*	74.69	98.36	87.50	62.50	93.85
2-	*Helicobacter pylori*	84.86	98.54	92.89	88.07	99.19
3-	*Bacillus cereus*	82.09	99.17	95.92	62.09	99.89
4-	*Staphylococcus aureus*	73.05	98.15	90.54	74.56	96.15

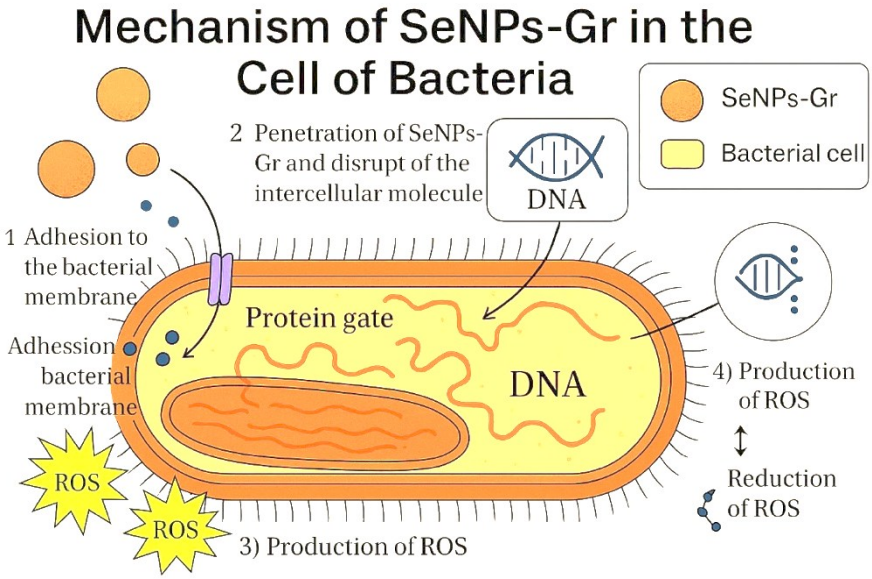

Fig. 9. The mechanism of SeNPs@Gr as an antibacterial on the bacterial cell wall

The peptidoglycan (murein) component of the bacterial cell wall was inhibited by the SeNPs-Gr, as shown in Fig. 9, which describes how the compound works. Bacteria classified as Gram-positive or Gram-negative have different amounts and locations of this polymer within their cell walls.

The antimicrobial activity of the nanoemulsions is attributed primarily to their ability to interact with and disrupt bacterial cell membranes through direct nanoparticle lipid interactions and membrane destabilization, rather than strong electrostatic attraction (Hwang *et al.* 2013). As indicated by the zeta potential analysis (Fig. 7b), the nanoparticles do not exhibit a pronounced cationic surface charge (Pisoschi *et al.* 2018). Consequently, membrane permeability changes, oxidative stress, and intracellular damage such as enzyme inactivation, leakage of essential biomolecules, and inhibition of nucleic acid and protein synthesis are considered the dominant mechanisms underlying the observed antibacterial effects (Pisoschi *et al.* 2018).

All of the aforementioned measures yielded outstanding antibacterial activity against the previously evaluated pathogenic strains. Lastly, samples 2 and 5 have a strong ability to reduce the number of Gram-positive bacteria (*Staphylococcus aureus* and *Bacillus cereus*) and Gram-negative bacteria (*Escherichia coli* and *Helicobacter pylori*). This makes them highly effective bactericidal agents. These samples have many potential uses in the medical and pharmaceutical fields, particularly as surgical burners and wound healing tools, as well as in food packaging and preservation. The colony-forming unit (CFU) reduction assay, which uses the shake flask method to identify bactericidal (≥99% CFU reduction) from bacteriostatic effects, was used to assess antimicrobial efficacy in place of the traditional broth dilution MIC/MBC assays.

Antioxidant

Antioxidant activity was assessed using the DPPH radical scavenging assay and expressed as percentage (%) inhibition. This approach was selected to allow direct comparison of the relative antioxidant performance of ginger oil, Gr-NE, and SeNPs@Gr under identical experimental conditions. A calibration curve using a reference antioxidant such as Trolox or ascorbic acid was not constructed in this study, and therefore, antioxidant

capacity was not expressed as equivalent units. While this limits direct quantitative comparison with other reports expressed as Trolox equivalents, the method remains suitable for comparative evaluation within the studied samples. This limitation is acknowledged, and future work will incorporate standard calibration curves to enable absolute antioxidant quantification. When compared to ginger oil, Gr-NE and SeNPs@Gr exhibited significantly different antioxidant properties, as shown by a comprehensive evaluation that was carried out with the use of the DPPH radical scavenging experiment (Table 3, Fig. S5).

Table 3. Samples' Antioxidant Activity Expressed as (%) Radical Scavenging Activity

Samples / Test volume (µL)		Treated sample (%) Radical Scavenging Activity					
		Trials			Mean	Standard deviation	Standard Error
		(1)	(2)	(3)			
1-	Gr-NE	69.43	79.12	80.89	76.48	5.04	2.91
2-	SeNPs@GR	87.56	88.56	89.8	88.64	0.92	0.53
3-	Ginger oil	29.63	33.94	38.59	34.05	3.66	2.11

Both SeNPs@Gr and Gr-NE demonstrated significantly increased activity, which highlights the significance that phytochemical composition plays in the antioxidant properties of nanoparticles generated from plants (Nawaz *et al.* 2019). The radical scavenging activity of SeNPs@Gr and Gr-NE was significantly increased. For biological applications, this finding emphasizes the great potential of selenium nanoparticles in ginger oil (SeNPs@Gr) and ginger oil nanoemulsion (Gr-NE) as antioxidant medicines. Because of their increased effectiveness, SeNPs@Gr and Gr-NE are good candidates for oxidative stress reduction in medicines, nutraceuticals, and personal care products. Their potential uses in preventing food spoilage and oxidative damage in a variety of formulations are supported by their strong antioxidant activity at high concentrations. In addition to its prospective applications in medicines, nutraceuticals, cosmetics, industrial and environmental domains, SeNPs@Gr shows promise as an excellent H scavenger.

Antioxidant Comparison

The radical scavenging assay was used in this investigation to measure the antioxidant activity. SeNPs@Gr had the highest scavenging activity (88.6%), followed by Gr-NE (76.5%), while ginger oil alone showed a relatively lower activity (34.0%), according to the results (Table 3). The SeNPs@Gr values were comparable to or better than many commonly reported natural antioxidants when compared to other studies. For example, the well-known antioxidant ascorbic acid (vitamin C) usually exhibits scavenging activity of 85 to 95%, contingent on assay conditions and concentration (Dahl *et al.* 2007; Paul *et al.* 2015). Under similar DPPH or radical scavenging tests, Trolox, a water-soluble vitamin E analogue, typically shows activity in the 80 to 90% range (Montgomery and Kroeger 1984). As a result, the SeNPs@Gr sample showed antioxidant efficacy on par with that of common antioxidants like vitamin C and Trolox, while Gr-NE also displayed strong activity, albeit at a slightly lower level. While essential oils typically have a weaker capacity to quench radicals than nanoparticle formulations, ginger oil alone demonstrated moderate scavenging activity (Balouiri *et al.* 2016). These comparisons demonstrate the

relative effectiveness of the newly synthesized samples and the improvement brought about by selenium functionalization and nano-formulation.

CONCLUSIONS

1. Selenium-based nanoparticles (SeNPs) were fabricated by means of a nanoemulsion (oil in water) of the environmentally friendly compound ginger oil.
2. The results revealed distinctive structural and optical characteristics, with ginger oil SeNPs exhibiting increased antibacterial and antioxidant capabilities. Significant antibacterial activity was exhibited by the SeNPs@Gr and ginger oil against a variety of pathogens. These microorganisms included Gram-positive bacteria such as *Staphylococcus aureus* and *Bacillus cereus*, as well as Gram-negative bacteria such as *Escherichia coli* and *Helicobacter pylori.*
3. The SeNPs@Gr and Gr-NE demonstrated significantly stronger antioxidant qualities than the ginger oil by itself, as demonstrated by the fact that they were able to scavenge DPPH through their activities.
4. The findings of this study shed light on the potential of ginger oil in the production of nanoparticles in a sustainable manner and lay the groundwork for further research into the application of plant-based nanotechnology in the field of biomedical research.

ACKNOWLEDGMENTS

The authors extend their appreciation to the Deanship of Research and Graduate Studies at the University of Tabuk for funding this work through Research No. S-0261-2024.

Conflict of Interest

The authors declare that they have no known competing financial interests or personal relationships that could have appeared to influence the work reported in this paper.

Statement of Ethics Approval

No animals or humans were used in our research work.

Data Availability Statement

The data presented in this study are available in the article.

REFERENCES CITED

Abdallah, A. B. E., El-Ghannam, M. A., Hasan, A. A., Mohammad, L. G., Mesalam, N. M., and Alsayed, R. M. (2023). "Selenium nanoparticles modulate steroidogenesis-related genes and improve ovarian functions *via* regulating androgen receptors expression in polycystic ovary syndrome rat model," *Biological Trace Element Research* 201, 5721-5733. https://doi.org/10.1007/s12011-023-03616-0

Afzal, M., Al-Hadidi, D., Menon, M., Pesek, J., and Dhami, M. S. I. (2001). "Ginger: An ethnomedical, chemical and pharmacological review," *Drug Metabolism and Drug Interactions* 18, 159-190. https://doi.org/10.1515/DMDI.2001.18.3-4.159

Al-Brakati, A., Alsharif, K. F., Alzahrani, K. J., Kabrah, S., Al-Amer, O., Oyouni, A. A., Habotta, O. A., Lokman, M. S., Bauomy, A. A., Kassab, R. B., and Abdel-Moneim, A. E. (2021). "Using green biosynthesized lycopene-coated selenium nanoparticles to rescue renal damage in glycerol-induced acute kidney injury in rats," *International Journal of Nanomedicine* 16, 4335-4349. https://doi.org/10.2147/IJN.S306186

Ali, B. H., Blunden, G., Tanira, M. O., and Nemmar, A. (2008). "Some phytochemical, pharmacological and toxicological properties of ginger (*Zingiber officinale* Roscoe): A review of recent research," *Food and Chemical Toxicology* 46, 409-420. https://doi.org/10.1016/j.fct.2007.09.085

Alkherb, W. A. H., Farag, S. M., Alotaibi, A. M., Aloui, Z., Alshammari, N. A. H., El-Sayed, A. A., Almutairi, F. M., and El-Shourbagy, N. M. (2024). "Synthesis and larvicidal efficacy of pyrazolopyrimidine derivatives conjugated with selenium nanoparticles against *Culex pipiens* L. and *Musca domestica* L. larvae," *Colloids and Surfaces B: Biointerfaces* 241, article 114040. https://doi.org/10.1016/j.colsurfb.2024.114040

Alrashdi, B. M., Fehaid, A., Kassab, R. B., Rizk, S., Habotta, O. A., and Abdel-Moneim, A. E. (2023). "Biosynthesized selenium nanoparticles using epigallocatechin gallate protect against pentylenetetrazole-induced acute epileptic seizures in mice via antioxidative, anti-inflammatory, and anti-apoptotic activities," *Biomedicines* 11, article 1955. https://doi.org/10.3390/biomedicines11071955

Amini, S. M., and Akbari, A. (2019). "Metal nanoparticles synthesis through natural phenolic acids," *IET Nanobiotechnol*. 13(8), 771-777. DOI: 10.1049/iet-nbt.2018.5386.

Anton, N., Benoit, J.-P., and Saulnier, P. (2008). "Design and production of nanoparticles formulated from nano-emulsion templates — A review," *Journal of Controlled Release* 128, 185-199. https://doi.org/10.1016/j.jconrel.2008.02.007

Badawy, M. E. I., Lotfy, T. M. R., and Shawir, S. M. S. (2019). "Preparation and antibacterial activity of chitosan–silver nanoparticles for application in preservation of minced meat," *Bulletin of the National Research Centre* 43, 1-14. https://doi.org/10.1186/S42269-019-0124-8

Balouiri, M., Sadiki, M., and Ibnsouda, S. K. (2016). "Methods for *in vitro* evaluating antimicrobial activity: A review," *Journal of Pharmaceutical Analysis* 6, 71-79. https://doi.org/10.1016/j.jpha.2015.11.005

Bhargav, H. S., Shastri, S. D., Poornav, S. P., Darshan, K. M., and Nayak, M. M. (2016). "Measurement of the zone of inhibition of an antibiotic," *Proceedings of the 6th International Advance Computing Conference (IACC 2016)*, 409-414. https://doi.org/10.1109/IACC.2016.82

Chaiyakunapruk, N., Kitikannakorn, N., Nathisuwan, S., Leeprakobboon, K., and Leelasettagool, C. (2006). "The efficacy of ginger for prevention of postoperative nausea and vomiting: A meta-analysis," *American Journal of Obstetrics and Gynecology* 194, 95-99. https://doi.org/10.1016/j.ajog.2005.06.046

Chrubasik, S., Pittler, M. H., and Roufogalis, B. D. (2005). "*Zingiberis rhizoma*: A comprehensive review on the ginger effect and efficacy profiles," *Phytomedicine* 12, 684-701. https://doi.org/10.1016/j.phymed.2004.07.009

Dahl, J. A., Maddux, B. L. S., and Hutchison, J. E. (2007). "Toward greener nanosynthesis," *Chemical Reviews* 107, 2228-2269. https://doi.org/10.1021/cr050943k

Diwu, W., Dong, X., Nasif, O., Alharbi, S. A., Zhao, J., and Li, W. (2021). "In-vivo

investigations of hydroxyapatite/co-polymeric composites coated titanium plate for bone regeneration," *Frontiers in Cell and Developmental Biology* 8, article 631107. https://doi.org/10.3389/fcell.2020.631107

El-Gohary, E. E., Farag, S. M., El-Sayed, A. A., Khattab, R. R., and Mahmoud, D. M. (2021). "Insecticidal activity and biochemical study of clove oil (*Syzygium aromaticum*) nano-formulation on *Culex pipiens* L. (Diptera: Culicidae)," *Egyptian Journal of Aquatic Biology and Fisheries* 25, 227-239. https://doi.org/10.21608/ejabf.2021.137233

Elmaaty, T. A., Sayed-Ahmed, K., Elsisi, H., Ramadan, S. M., Sorour, H., Magdi, M., and Abdeldayem, S. A. (2022). "Novel antiviral and antibacterial durable polyester fabrics printed with selenium nanoparticles (SeNPs)," *Polymers* 14, article 955. https://doi.org/10.3390/polym14050955

El-Masry, H. M., Atwa, N. A., El-Beih, A. A., Agwa, M. M., Khafagi, I. K., Mansour, S. R., and El-Diwany, A. I. (2023). "Phenazine-producing *Pseudomonas aeruginosa* OQ158909: A promising candidate for biological activity and therapeutic applications," *Egyptian Journal of Chemistry* 66, 281-303. https://doi.org/10.21608/ejchem.2023.214109.8045

El-Sayed, A. A., Abu-Bakr, S. M., Swelam, S. A., Khaireldin, N. Y., and Shoueir, K. R., Khalil, A. M. (2022). "Applying nanotechnology in synthesis of benzimidazole derivatives: A pharmacological approach," *Biointerface Research in Applied Chemistry* 12, 992-1005. https://doi.org/10.33263/BRIAC121.9921005

Fryd, M. M., and Mason, T. G. (2012). "Advanced nanoemulsions," *Annual Review of Physical Chemistry* 63, 493-518. https://doi.org/10.1146/annurev-physchem-032210-103436

Grzanna, R., Lindmark, L., and Frondoza, C. G. (2005). "Ginger — An herbal medicinal product with broad anti-inflammatory actions," *Journal of Medicinal Food* 8, 125-132. https://doi.org/10.1089/jmf.2005.8.125

Gupta, A., Eral, H. B., Hatton, T. A., and Doyle, P. S. (2016). "Nanoemulsions: Formation, properties and applications," *Soft Matter* 12, 2826-2841. https://doi.org/10.1039/C5SM02958A

Hafez, A. I., Ali, H. M., Sabry, R. M., El-Masry, H. M., and Abd El-Gawad, W. M. (2023). "Generation of novel, hygienic, inhibitive, and cost-effective nanostructured core-shell pigments," *Progress in Organic Coatings* 175, article 107325. https://doi.org/10.1016/J.PORGCOAT.2022.107325

Hamoda, D. M., Kenawy, S. H., Aboalmaged, H. H., Rashed, U. M., Almetwally, A. A., and El-Masry, H. M. (2022). "Plasma technique application for coating non-woven fabric by ($CaSiO_3$/CuO) nanoparticles for biomedical sector," *Egyptian Journal of Chemistry* 65, 773-778. https://doi.org/10.21608/EJCHEM.2022.128815.5705

Hwang, Y. Y., Ramalingam, K., Bienek, D. R., Lee, V., You, T., and Alvarez, R. (2013). "Antimicrobial activity of nanoemulsion in combination with cetylpyridinium chloride in multidrug-resistant *Acinetobacter baumannii*," *Antimicrobial Agents and Chemotherapy* 57, 3568-3575. https://doi.org/10.1128/AAC.02109-12

Jacob, J. A., Mahal, H. S., Biswas, N., Mukherjee, T., and Kapoor, S. (2007). "Role of phenol derivatives in the formation of silver nanoparticles," *Langmuir* 24(2), 528-533. https://doi.org/10.1021/la702073r

Kamal, G. M., Nazi, N., Sabir, A., Saqib, M., Zhang, X., Jiang, B., Khan, J., Noreen, A., Uddin, J., and Murtaza, S. (2023). "Yield and chemical composition of ginger essential oils as affected by inter-varietal variation and drying treatments of rhizome,"

Separations 10, article 186. https://doi.org/10.3390/SEPARATIONS10030186

Kamel, O. M. H. M., El-Halim, M. D. A., Khalil, A. M., Elasasy, M. E. A., and El-Sayed, A. A. (2024). "A promising route to control mosquito larvae by metal nanoparticles," *Egyptian Journal of Aquatic Biology and Fisheries* 28, 1699-1732.

Khan, S. A., and Lee, C. S. (2020). "Recent progress and strategies to develop antimicrobial contact lenses and lens cases for different types of microbial keratitis," *Acta Biomaterialia* 113, 101-118. https://doi.org/10.1016/j.actbio.2020.06.039

Khattab, R. R., Swelam, S. A., Khalil, A. M., Abdelhamid, A. E., Soliman, A. M., and El-Sayed, A. A. (2021). "Novel sono-synthesized triazole derivatives conjugated with selenium nanoparticles for cancer treatment," *Egyptian Journal of Chemistry* 64, 4675-4688. https://doi.org/10.21608/ejchem.2021.81154.4018

Kumar, M., Misra, A., Babbar, A. K., Mishra, A. K., Mishra, P., and Pathak, K. (2008). "Intranasal nanoemulsion based brain targeting drug delivery system of risperidone," *International Journal of Pharmaceutics* 358, 285-291. https://doi.org/10.1016/j.ijpharm.2008.03.029

Landfester, K. (2009). "Miniemulsion polymerization and the structure of polymer and hybrid nanoparticles," *Angewandte Chemie International Edition* 48, 4488-4507. https://doi.org/10.1002/anie.200900723

Liu, X., Sun, J., Du, J., An, J., Li, Y., Hu, Y., Xiong, Y., Yu, Y., Tian, H., Mei, X., and Wu, C. (2023). "Encapsulation of selenium nanoparticles and metformin in macrophage-derived cell membranes for the treatment of spinal cord injury," *ACS Biomaterials Science & Engineering* 9, 5709-5723. https://doi.org/10.1021/acsbiomaterials.3c01009

Lovelyn, C., and Attama, A. A. (2011). "Current state of nanoemulsions in drug delivery," *Journal of Biomaterials and Nanobiotechnology* 2, 626-639. https://doi.org/10.4236/jbnb.2011.225075

Manojlović-Stojanoski, M., Borković-Mitić, S., Nestorović, N., Ristić, N., Trifunović, S., Stevanović, M., Filipović, N., Stojsavljević, A., and Pavlović, S. (2022). "The effects of BSA-stabilized selenium nanoparticles and sodium selenite supplementation on the structure, oxidative stress parameters and selenium redox biology in rat placenta," *International Journal of Molecular Sciences* 23, article 13068. https://doi.org/10.3390/ijms232113068

Mason, T. G., Wilking, J. N., Meleson, K., Chang, C. B., and Graves, S. M. (2006). "Nanoemulsions: formation, structure, and physical properties," *Journal of Physics: Condensed Matter* 18, article R635. https://doi.org/10.1088/0953-8984/18/41/R01

McClements, D. J. (2011). "Edible nanoemulsions: Fabrication, properties, and functional performance," *Soft Matter* 7, 2297-2316. https://doi.org/10.1039/c0sm00549e

Montgomery, E. H., and Kroeger, D. C. (1984). "Principles of anti-infective therapy," *Dental Clinics of North America* 28, 423-432. https://doi.org/10.1016/B978-0-323-50934-3.00008-2

Nawaz, H., Waheed, R., and Nawaz, M. (2019). "Phytochemical composition, antioxidant potential, and medicinal significance of *Ficus*," *Modern Fruit Industry (IntechOpen)*. https://doi.org/10.5772/intechopen.86562

Oktay, M., Gülçin, I., and Küfrevioğlu, Ö. I. (2003). "Determination of *in vitro* antioxidant activity of fennel (*Foeniculum vulgare*) seed extracts," *LWT – Food Science and Technology* 36, 263-271. https://doi.org/10.1016/S0023-6438(02)00226-8

Osman, H. H., Abdel-Hafez, H. F., and Khidr, A. A. (2015). "Comparison between the

efficacy of two nanoparticles and effective microorganisms on some biological and biochemical aspects of *Spodoptera littoralis*," *International Journal of Agricultural Innovation and Research* 3, 1620-1626.

Paul, J. A. J., Selvi, B. K., and Karmegam, N. (2015). "Biosynthesis of silver nanoparticles from *Premna serratifolia* L. leaf and its anticancer activity in CCl_4-induced hepato-cancerous Swiss albino mice," *Environmental Chemistry Letters* 13, 1-10. https://doi.org/10.1007/s13204-014-0397-z

Pisoschi, A. M., Pop, A., Georgescu, C., Turcuş, V., Olah, N. K., and Mathe, E. (2018). "An overview of natural antimicrobials role in food," *European Journal of Medicinal Chemistry* 143, 922-935. https://doi.org/10.1016/j.ejmech.2017.11.095

Ramadan, M. E., El-Saber, M. M., Abdelhamid, A. E., and El-Sayed, A. A. (2022). "Effect of nano-chitosan encapsulated spermine on growth, productivity and bioactive compounds of chili pepper (*Capsicum annuum* L.) under salinity stress," *Egyptian Journal of Chemistry* 65, 197-207. https://doi.org/10.21608/ejchem.2021.105793.4870

Ravi Kiran, T., and Aruna, H. K. (2010). "Antioxidant enzyme activities and markers of oxidative stress in the life cycle of earthworm, *Eudrilus eugeniae*," *Italian Journal of Zoology* 77, 144-148. https://doi.org/10.1080/11250000902932841

Sarker, D. (2005). "Engineering of nanoemulsions for drug delivery," *Current Drug Delivery* 2, 297-310. https://doi.org/10.2174/156720105774370267

Shakeel, F., Baboota, S., Ahuja, A., Ali, J., Aqil, M., and Shafiq, S. (2007). "Nanoemulsions as vehicles for transdermal delivery of aceclofenac," *AAPS PharmSciTech* 8, article 191. https://doi.org/10.1208/pt0804104

Shinde, V., and Desai, K. (2022). "*In vitro* cytotoxicity, macromolecular interaction and antioxidant potential of dual coated selenium nanoparticles," *Journal of Biomedical Materials Research Part B: Applied Biomaterials* 110, 1400-1411. https://doi.org/10.1002/jbm.b.35008

Shukla, Y., and Singh, M. (2007). "Cancer preventive properties of ginger: A brief review," *Food and Chemical Toxicology* 45, 683-690. https://doi.org/10.1016/j.fct.2006.11.002

Solans, C., Izquierdo, P., Nolla, J., Azemar, N., and Garcia-Celma, M. J. (2005). "Nano-emulsions," *Current Opinion in Colloid & Interface Science* 10, 102-110. https://doi.org/10.1016/j.cocis.2005.06.004

Spyridopoulou, K., Aindelis, G., Pappa, A., and Chlichlia, K. (2021). "Anticancer activity of biogenic selenium nanoparticles: Apoptotic and immunogenic cell death markers in colon cancer cells," *Cancers* 13, article 5335. https://doi.org/10.3390/cancers13215335

Tadros, T., Izquierdo, P., Esquena, J., and Solans, C. (2004). "Formation and stability of nano-emulsions," *Advances in Colloid and Interface Science* 108–109, 303-318. https://doi.org/10.1016/j.cis.2003.10.023

Tohamy, H. A. S., and El-Masry, H. M. (2024). "Fluffy-like amphiphilic graphene oxide and its effects on improving the antibacterial activity and thermal outstanding of ethyl cellulose/polyvinyl alcohol hydrogel film," *BMC Chemistry* 18, 1-9. https://doi.org/10.1186/S13065-024-01221-3

Article submitted: November 30, 2025; Peer review completed: January 18, 2026; Revised version received and accepted: January 21, 2026; Published: February 27, 2026.
DOI: 10.15376/biores.21.2.3569-3592

APPENDIX

Table S1. Zeta Potential and Particle Size of Ginger Nano-emulsion

Compound	MPS (nm)	PDI	SD	Zeta Potential
Gr-NE	194.8	0.624	±5.624	-33.3

Figure S1 shows the UV-VIS absorption spectra of the selenium nanoparticles that were synthesized. In a colloidal solution containing selenium nanoparticles, a UV-Vis absorption peak maximum at 460 nm was noticed, suggesting the existence of surface plasmon resonance peaks. Because they didn't seem to aggregate, this indicates that the nanoparticles were successfully manufactured and dispersed uniformly throughout the water solution (Dahl *et al.* 2007; Paul *et al.* 2015).

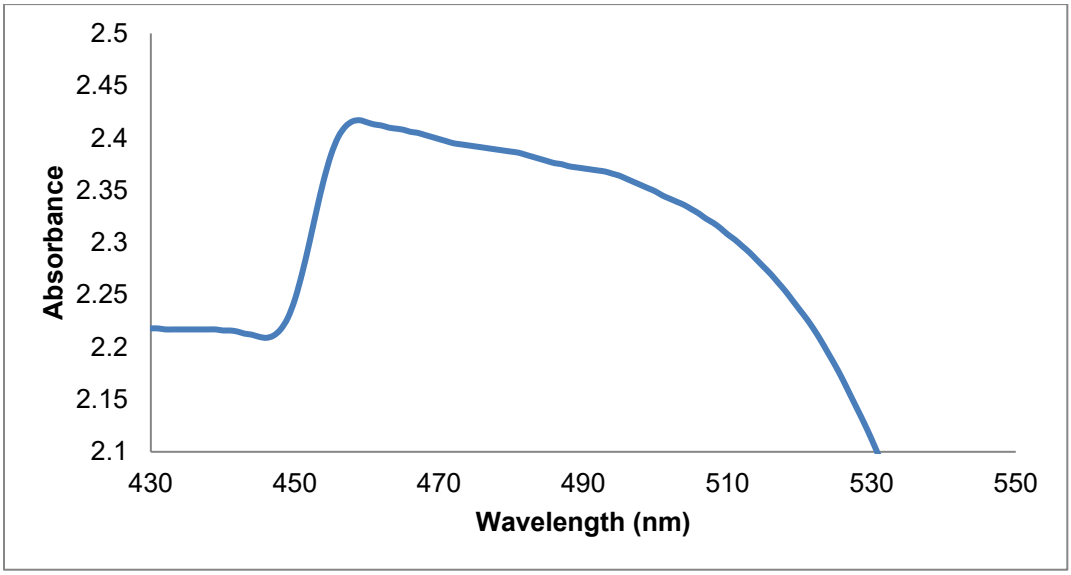

Fig. S1. UV-VIS spectra of SeNPs@*Gr*

Table S2. Particle Size and Zeta Potential of SeNPs@Gr

Compound	MPS (nm)	PDI	SD	Zeta Potential
Gr@SeNPs	55.74	0.528	±6.734	-8.05

Table S3. Main Particle Size from the TEM Measurements

Characterization Method	Mean Particle Size (nm) ± SD	Notes / Significance
TEM Gr@SeNPs	76.7 ± 14.3 (n = 4)	Physical “dry” size confirms morphology and nanoscale structure
Gr-NE	40.94 ±6.82 (n = 4)	Physical “dry” size confirms morphology and nanoscale structure

Table S4. Active Compounds of Ginger Oil by GC-MS

Peak	RT	Name	Formula	Area	Area %
1	7.971	trans-.beta.-Ocimene	$C_{10}H1_6$	3735472.03	0.8
2	8.24	Camphene	$C_{10}H1_6$	15769058.9	3.38
3	11.562	Isoborneol	$C_{10}H_{18}O$	4309382.72	0.92
4	14.327	.beta.,.epsilon.-Carotene-3,3'-diol, (3R,3'R,6'R)-	$C_{40}H_{56}O_2$	3649272.28	0.78
5	15.321	Benzene, 1-(1,5-dimethyl-4-hexenyl)-4-methyl- (α-Curcumin)	$C_{15}H_{22}$	171350464	36.75
6	15.459	(R)-1-Methyl-4-(6-methylhept-5-en-2-yl)cyclohexa-1,4-diene (β-Curcumin)	$C_{15}H_{24}$	91182622	19.55
7	15.621	1H-Benzocycloheptene, 2,4a,5,6,7,8,9,9a-octahydro-3,5,5-trimethyl-9-methylene-, (4aS-cis)-	$C_{15}H_{24}$	66890756.1	14.34
8	15.684	.gamma.-Muurolene	$C_{15}H_{24}$	29377348.8	6.3
9	15.828	.beta.-Longipinene	$C_{15}H_{24}$	71324773.3	15.3
10	17.592	2-Butanone, 4-(4-hydroxy-3-methoxyphenyl)-	$C_{11}H_{14}O_3$	5336569.25	1.14
11	20.494	geranyl-.alpha.-terpinene	$C_{20}H_{32}$	3392129.43	0.73
Total percent					99.99

GC-MS for Ginger Oil

According to the published references [12,13], the compounds containing β and α-curcumin were identified by GC-MS analysis of ginger essential oil. benzene, 1-(1,5-dimethyl-4-hexenyl)-4-methyl, which is equivalent to α-curcumin (also called ar-curcumene). According to earlier reports, this compound is a significant component of ginger essential oil, especially in oven-dried samples where it made up around 9.4% of the total composition [12]. The chemical identity of α-curcumene is well-characterized in reference databases, where it is referred to as (R)-1-Methyl-4-(6-methylhept-5-en-2-yl)cyclohexa-1,4-diene (β-Curcumin) and 1-(1,5-dimethyl-4-hexenyl)-4-methyl benzene (α-curcumin). These results support our GC-MS conclusions and are consistent with previous research on the volatile profile of ginger.

Antimicrobial Activity

The agar well diffusion method was initially used to assess the tested samples' antimicrobial properties (Table 1). Ginger oil alone and SeNPs showed limited or no activity, whereas both SeNPs@Gr (sample 2) and ginger oil/DMSO (sample 5) produced clear inhibition zones against *Escherichia coli, Helicobacter pylori, Bacillus cereus, and Staphylococcus aureus*. The inhibition zones showed encouraging activity, especially against *H. pylori* and *B. cereus*, despite being smaller than those generated by the reference antibiotic gentamicin (10 µg/disc). Bacterial viability after treatment was assessed using the shake flask method in order to confirm and measure the antimicrobial effect (Table 2). In this case, the difference between bactericidal and bacteriostatic actions became evident. In samples 1, 3, and 4, Gr-NE, SeNPs, and ginger oil all decreased viable counts to varied degrees (62 to 95%), which is in line with a bacteriostatic effect. However, SeNPs@Gr and ginger oil/DMSO (samples 2 and 5) were classified as bactericidal agents because they reduced colony-forming units (CFU) by 96 to 99% in both Gram-positive (*B. cereus, S. aureus*) and Gram-negative (*E. coli, H. pylori*) strains. Crucially, SeNPs@Gr's bactericidal action is comparable to gentamicin's effectiveness, indicating its potential as a natural antimicrobial substitute.

SeNPs@Gr interacts mechanistically with the lipid bilayer and peptidoglycan layer of bacterial cell walls, as shown in Fig. 6. Adhesion and membrane fusion are facilitated by electrostatic interactions between the negatively charged bacterial surface and the cationic nanoparticles (Hwang *et al.* 2013). Essential biomolecules leak out as a result of this destabilisation, which also damages membrane integrity and increases permeability. Inhibition of protein and nucleic acid synthesis, inactivation of enzymes, and breakdown of the proton motive force are subsequent intracellular effects (Pisoschi *et al.* 2018). Therefore, the combined effect of physically disrupting bacterial envelopes and interfering with essential metabolic pathways can be responsible for the significant bactericidal activity seen for SeNPs@Gr and ginger oil/DMSO. Altogether, these findings offer mechanistic and descriptive proof of antimicrobial activity. The activity of the nanoformulations is confirmed by benchmarking against gentamicin, and the CFU reduction assays offer a numerical assessment of dose-response. SeNPs@Gr's dual mechanism of action—intracellular damage and membrane disruption emphasizes its potential as a multipurpose antimicrobial agent with uses in medicine, wound care, and food preservation.

Fig. S2. Antimicrobial activities of Gr-NE, SeNPs@Gr, Oil, Oil 50%

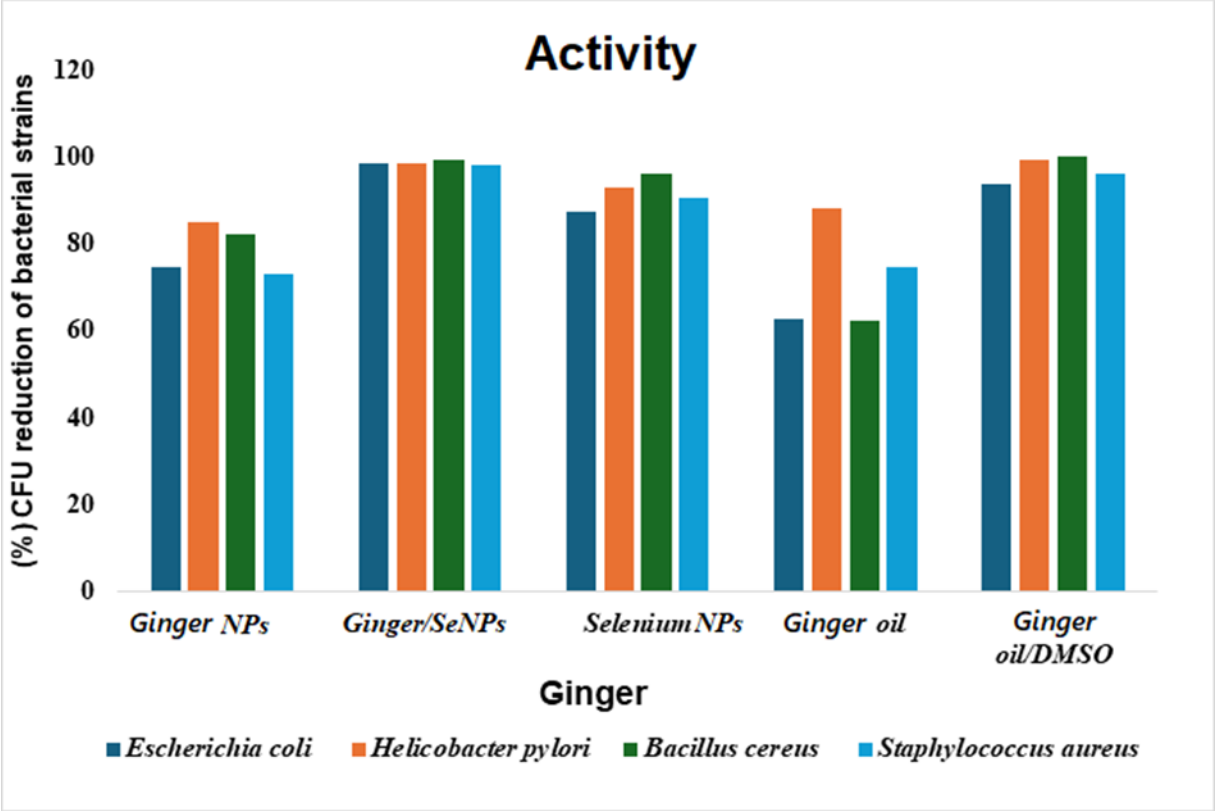

Fig. S3. Evaluation of Gr-NE, SeNPs@Gr, and Ginger oil antibacterial properties using the shake flask method

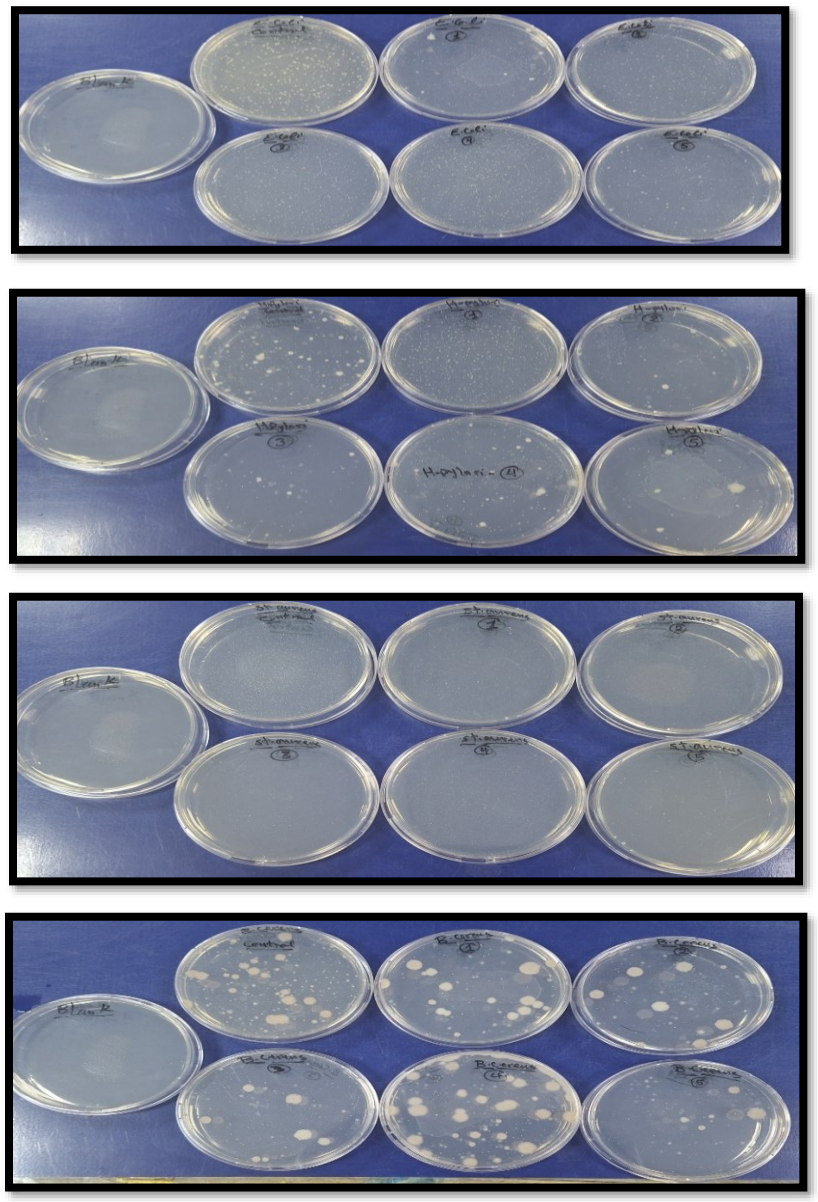

Fig. S4. CFU of bacterial strains

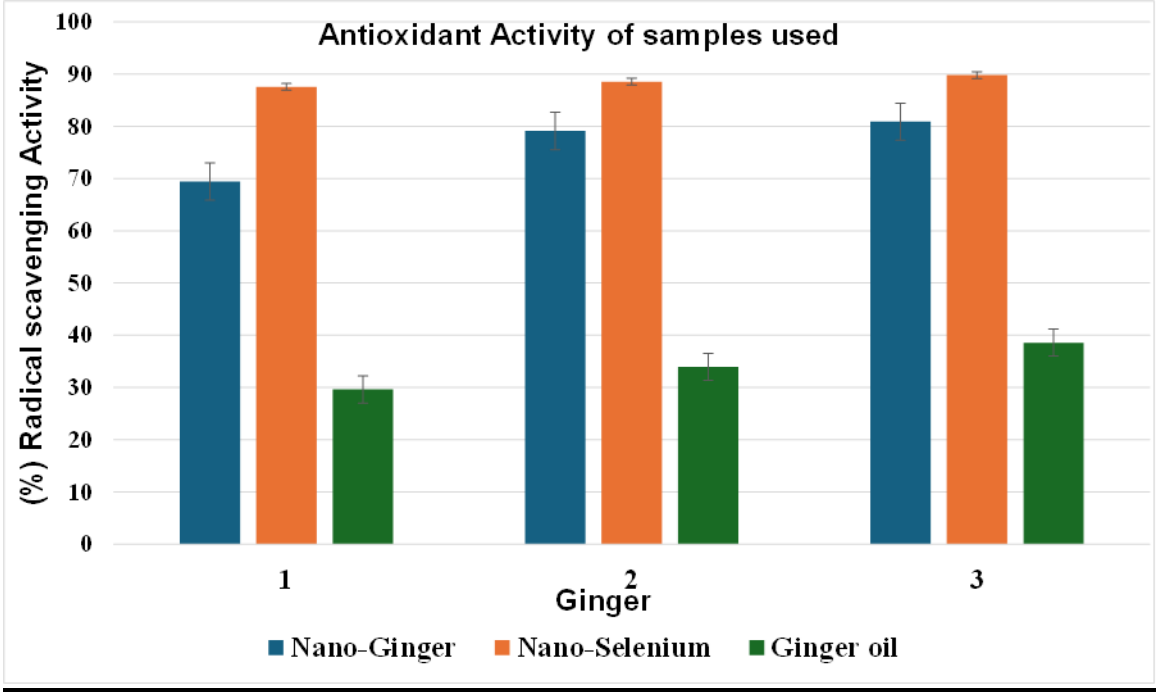

Fig. S5. Evaluation of Gr-NE, SeNPs@Gr, and Ginger oil antioxidant properties